Asociación Argentina de Mecánica Computacional

Mecánica Computacional Vol XXIX, págs. 7223-7236 (artículo completo)
Eduardo Dvorkin, Marcela Goldschmit, Mario Storti (Eds.)
Buenos Aires, Argentina, 15-18 Noviembre 2010

STRESSES ANALYSIS AND VERIFICATION OF THE WEB WELD CONNECTION OF OPENED I-BEAM IN COMPOSITE CONSTRUCTION

Otávio Cavalcante[a], Luciano Bezerra[b] and Cleirton Freitas[b]

[a]*Universidade Federal do Cerá- Campus Cariri, Juazeiro do Norte, otaviorc@hotmai.com*

[b]*Universidade de Brasília Brasília, lmbz@unb.br*

Keywords: Composite beam, Open-web, Composite Construction, Steel and Concrete.

Abstract. Composite construction may be a solution that makes possible the exploration of the maximum strength of the two main materials used in civil construction; concrete and steel. In some situations, due to architectural or weight optimization reasons, the steel I-beams used in such composite construction have patterns of holes in their webs. The I-beam may be produced from two 'T" steel rolled sections welded by their webs after the hole pattern is cut off. The connecting weld is located in the middle of the resultant I-beam web and matches the neutral axis of such beam. When used in composite construction, due to the concrete slab, the neutral axis of the steel I-beam is displaced upwards producing in the weld higher stresses. There is no recommendation from the standards guiding the verification against collapse of such web weld. This paper presents a numerical study of the stresses acting in the weld line of I-beam with hole pattern used in composite construction. The study was performing using a Finite Element model. The model discrete the steel I-beam and the concrete effective slab. Perfect link between concrete slab and steel beam is assumed. The 3D FE analyses take into account the size and the spacing of the holes in the I-beam web. The FE results show the minimum weld length that might resist the stresses on the weld line of the open I-beam. Conclusions and suggestions for future work are also present.

1 INTRODUCTION

Composite beam system with holes in the web has the advantage of reducing the beam weight and, moreover, the holes allow ducts to pass through the beam web. Different hole patterns offer diverse design options to architects. The composite I-beam analyzed in this article has hexagonal hole pattern produced from zigzag cuts of period (P) along the span of a rolled I-Beam with full-web (here named "original IB") as shown in Figure-1a and 1b. After the cuts, two rolled "T" beams are formed. One of the "T" section may be rotated (Figure 1a) or displaced (Figure 1b) to produce the desired hexagonal hole pattern of the new open-web I-beam (Figure 1). For simplification, this new Hexagonal open-web I-Beam hereafter is named "HoIB". Comparing the two procedures illustrated in Figure 1a and 1b, the first process produces a more efficient beam - since at the ends of the resultant beam, more web material is available and, consequently, a better shear resistance is obtained. The new HoIB section in Figure-1 is taller than the original IB. The increase in the height (and as a result an increase in the flexural resistance) is achieved without adding any steel material; thus, HoIB has the same weight of the original IB.

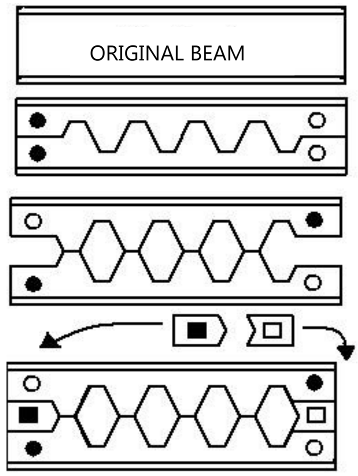

(a) Top "T" section is rotated

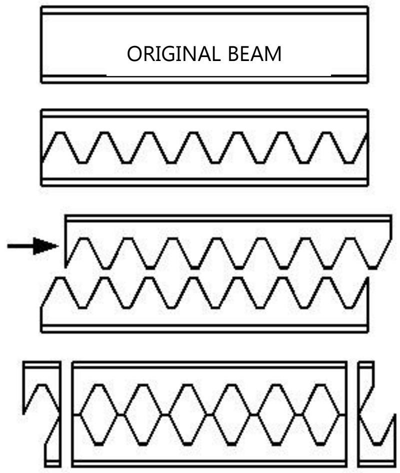

(b) Top "T" section is displaced

Figure 1: Examples of manufacturing open-web I sections

1.1 Holes size

I The hexagonal hole geometry considered in the beam in Figure 1 follows the recommendations by Cimadevila (2000), in which the hexagonal base (L_1, in Figure 2) is half the size of the hexagon length (L_1+2L_2). The resultant beam is twice higher than the hole height (h_f), as recommended by Standards (NBR-8800 (2003)). Taking these two parameters (L_1, h_f) and Figure 2; it is possible to know the final beam depth (h_{p1}) and the depth of the hole cut (h_c) from the original steel section. hp1 and hc, respectively, are expressed by the following Equations

$$\left|\begin{array}{l} h_{p1} = h_{po} + h_c \\ h_f = 2.h_c \\ h_f = n.h_{p1} \\ n \le 0,5 \end{array}\right. \qquad h_{p1} = h_{po} + \frac{n.h_{p1}}{2} \quad \Rightarrow \quad h_{p1} = \frac{2.h_{po}}{(1-n)} \tag{1}$$

$$\left|\begin{array}{l} h_{p1} = h_{po} + h_c \\ h_f = 2.h_c \\ h_{po} = n.h_{p1} \\ n \le 0,5 \end{array}\right. \qquad \frac{h_f}{n} = h_{po} + h_c \quad \Rightarrow \quad h_c = \frac{n.h_{po}}{(2-n)} \tag{2}$$

1.2 Slab influence

After the assemblage of the new HoIB, the connecting weld between the two "T" sections (Figure 1) will be at the centre line. The weld position coincides with the neutral axis (NA) of the new HoIB section. However, when this new HoIB is used in a composite construction (due to the concrete slab) the NA moves towards the concrete slab. This fact produces higher stresses in the welding region (Figure-3 and 5). Considering a complete interaction between concrete and steel section, the composite beam using the new HoIB may have the NA located on: (a) the concrete slab, or (b) the HoIB flange, or (c) the I-beam web. According to the Standards (NBR-8800 (2003)) the NA location in section A-A (Figure 2) may be determined according to the following equations:

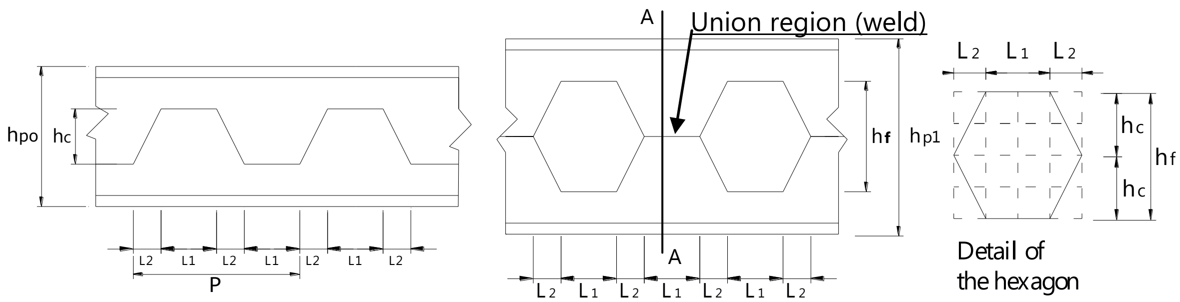

Figure 2: Details of the steel structure and the hole

a) For NA on the concrete slab and $\gamma_c.(0,85.A_c.f_{cck}) \ge \gamma_s.(A_s.f_y)$. (Fig.3a)

$$y = \frac{\gamma_s.A_s.f_y}{\gamma_c.0,85.f_{cck}.b_e} \tag{3}$$

b) For NA on the I-beam flange and $\gamma_c.(0,85.A_c.f_{cck}) \ge \gamma_s.(A_s - 2.b_f.t_f).\ f_y$ (Fig.3b)

$$y = \frac{\gamma_s.A_s.f_y - \gamma_c.(0{,}85.A_c.f_{cck})}{2.b_f.\gamma_s.f_y} \qquad (4)$$

c) For NA on the I-beam web and $\gamma_c.(0{,}85.A_c.f_{cck}) < \gamma_s.(A_s - 2.b_f.t_f).f_y$ (Fig.3c)

$$y = t_f + \frac{\gamma_s.A_s.f_y - \gamma_c.0{,}85.f_{cck}.A_c - \gamma_c.2.b_f.t_f.f_y}{\gamma_s.2.t_w.f_y} \qquad (5)$$

Where 0,85 is due to Rüsh's effect (NBR- 8800 (2003)), γ_c = resistance factor for concrete = 1/1,4 (MacGregor (1992)), γ_s = resistance factor for steel =1/1,15(Galambos (1996)), Ac = concrete area, As = steel section area, bf = flange width, f_{cck} = compressive stress for concrete (here taken as f_{cck}=25MPa), f_y = yield stress for steel (here considered as f_y=250MPa), b_f = flange width, t_f = flange thickness, and t_w = web thickness. Figure 3 shows all these parameters.

Considering Equations (3) to (5), and section A-A of Figure 2, the NA moves as a function of the concrete slab (CS) area. Figure-4 shows the change of position of the NA of the new HoIB towards the CS. The origin of the plot in Figure 4 corresponds to the NA position aligned to the centre of the new HoIB when no CS is considered. To obtain that plot in Figure-4, increments of 1cm is added to the CS width (b_e) and Equations (3) to (5) are taken into account. In this work the slab thickness is t_c =10cm, and the original IB is a rolled beam W 200x15 (with hpo = 20cm; b_f = 10cm; t_f = 0,52cm, and t_w = 0,43cm) – symbols are explained in Figure-3.

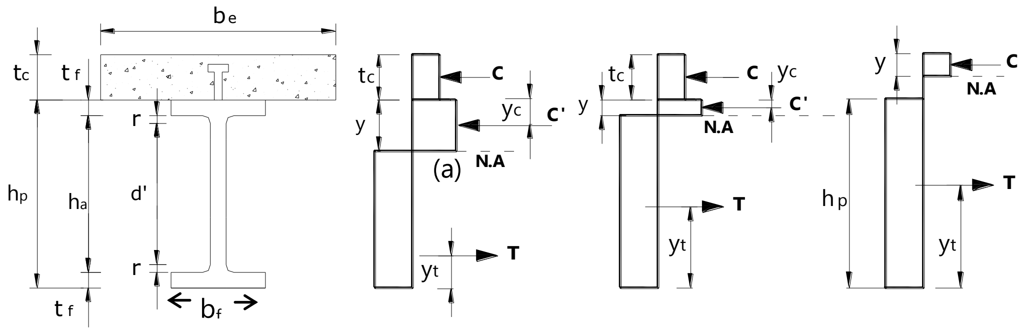

Figure 3: Forces on the section and at the weld region

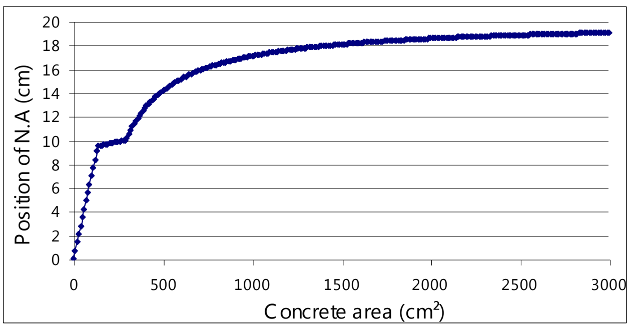

Figure 4: Position of the NA as a function of the CS area

If the NA (Figure-3a, b, and c) is in the CS, the whole steel HoIB section is under tension, this may represent an increment in the strength of the beam. Although at the weld region (Figure 2) a higher state of stress on the weld may be formed due to the displacement of the NA towards the CS (d_1 in Figure 5). This figure also illustrates the stress distribution in hybrid composite beam where no interaction between concrete and steel is verified (Figure 5b). "x_1" represents the normal stress along the weld string.

The stress state created at the weld region, may generate failure of the weld. This paper focuses on the stresses acting on the weld string under several aspects including beam span, weld length (L_1), and the displacement of the NA.

2 NUMERICAL ANALYSIS

The stress on the weld are determined numerically with 3D FEM models. The software "ANSYS" is used and this study is limited to composite beams simply supported at the ends, and under uniform loading along the beam spans. Due to the symmetries of geometry and loading in the composite HoIB only one quarter of composite beam could be discretized to reduce computational time. Half of the beam span is used but despite the symmetry of the cross section, the discretization of the whole section is adopted. This is done with the intention to avoid undesirable stress concentration due to the imposition of the appropriate displacement constrained at the nodes in the line of symmetry at the cross section. The cross section is the W200x15 and at the support region a steel bearing plate is used so that excessive deformation and stress concentration are also avoided.

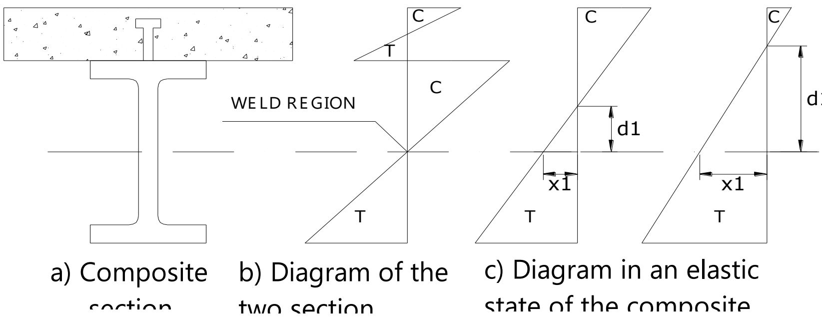

Figure 5: Stress at the cross section as a function of the NA displacement

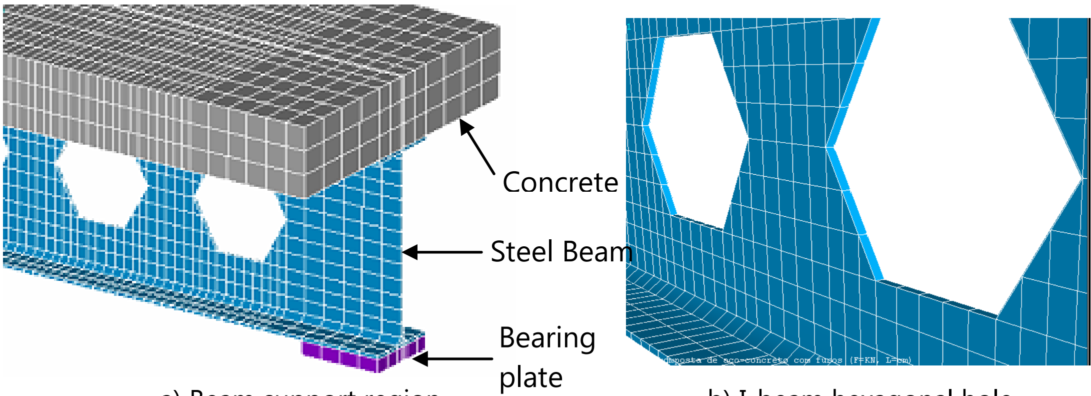

a) Beam support region b) I-beam hexagonal hole

Figure 6: Part of the 3D FE mesh of the composite HoIB

A 3D solid finite element, named SOLID-45, from ANSYS's element library is used to represent the steel HoIB and the bearing plate. The characteristics of such element are illustrated in Figure-7 and in Table 1. The 3D finite element, named SOLID-65, also from the ANSYS's element library is employed to discretize the concrete slab. This finite element is similar to SOLID-45, and the main characteristics may also be read in Figure-7 and in Table 1. The major difference between SOLID-45 and 65 is because the later offers cracking and crushing capabilities which make possible the appropriate simulation of the concrete nonlinearities.

Number of nodes	8
Node's connectivity	I, J, K, L, M, N, O, P
Degrees of freedom per node	Ux, Uy, Uz
Engineering applications	Structural, Mechanical, etc..

Table 1: Main characteristics for elements SOLID-45 and 65 (ANSYS user manual(1995)).

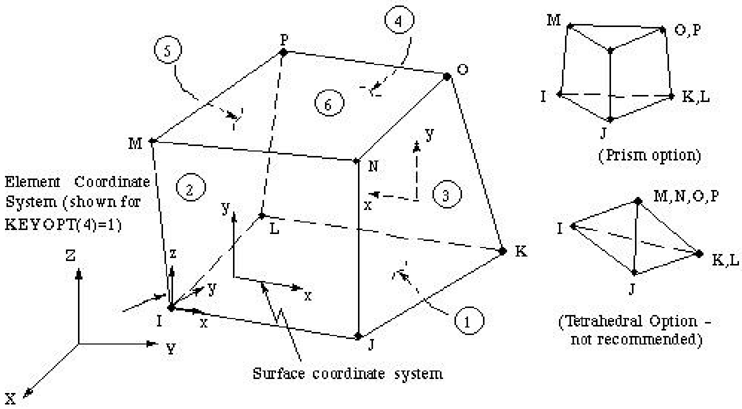

Figure 7: SOLID-45 and SOLID-65 connectivity and shapes (ANSYS user manual(1995)).

Structure's Face	Restriction direction of the points in the Figure-8	
	Filed	Not filed
Support region	Ux,Uy,Uz	Ux
Mid- span	-	Ux, Uy

Table 2: Constraints applied at nodes marked with circles in Figure8

2.1 Boundary conditions

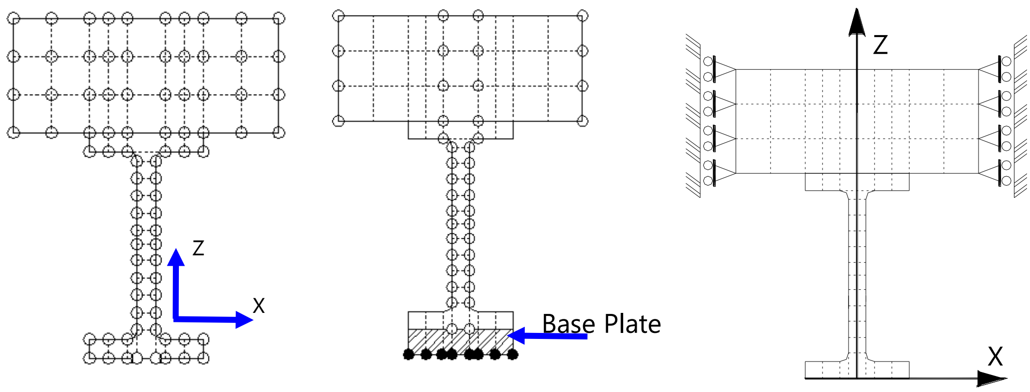

a) Mid span region b) Support region c) CS boundary condition

Figure 8: Representation of the constraints nodes in a composite section.

The beams investigated in this paper are all simply supported. X and Y axis are in cross section plane while the Y-axis is along the span, see Figure 8. To avoid unsymmetrical displacements of the cross section at the ends and at the middle of the beam span, some displacement constraints are applied. Figure-8 shows the nodes (with solid or hollow circles) where the displacement constraints are imposed according to the specifications in Table 2. Also at the ends of the beam the constraints representing the simple support condition are imposed. To force the CS to displace ideally without any possibility of lateral displacement, constraints inhibiting lateral displacements but allowing vertical movement of the beam is imposed in the CS as represented in Figure 8c.

3 ANALYTICAL APPROACH

In this model, it is assumed that the compression forces (F_c) are limited to the CS area and the tension forces (F_t) are given by the inferior rolled "T" section making up the HoIB steel section. From the bottom to top, by equilibrium, $F_t = F_s$. Considering the moment generated by the couple F_c and F_t which is in equilibrium at point A to the couple created by Q w.r.t. point A, we may write that F_s = Qp/d Therefore, the shearing stress in the weld (τ_w) (see Figure 9), may be expressed by Equation (6).

$$\tau_w = \frac{F_s}{L_1.t_w} = \frac{Q.p}{d_0.(L_1.t_w)} = \frac{Q}{d_0.t_w}.\left(\frac{2.(L_1+L_2)}{L_1}\right) \Rightarrow \quad \tau_w = \frac{Q}{d_0.t_w}.k \qquad (6)$$

3.1 Model – 02

The second model assumes the moment (M) equilibrium an point “A” (Figure-10b):

$$\sum M = 0 \therefore F_S.V_a - \left(\frac{Q+F}{2}\right).\frac{P}{2} - \left(\frac{Q}{2}\right).\frac{P}{2} = 0 \quad \therefore F_S = \left(Q+\frac{F}{2}\right).\frac{P}{2.V_a} \qquad (7)$$

In this case, the shearing stress in the weld (τ_w) is:

$$\tau_W = \frac{F_S}{L_1.e_W} \therefore \tau_S = \frac{F_S}{A_W} \qquad (8)$$

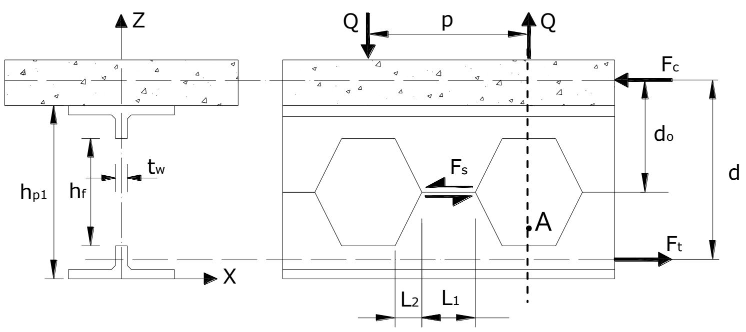

Figure 9: Forces in equilibrium in Model-01.

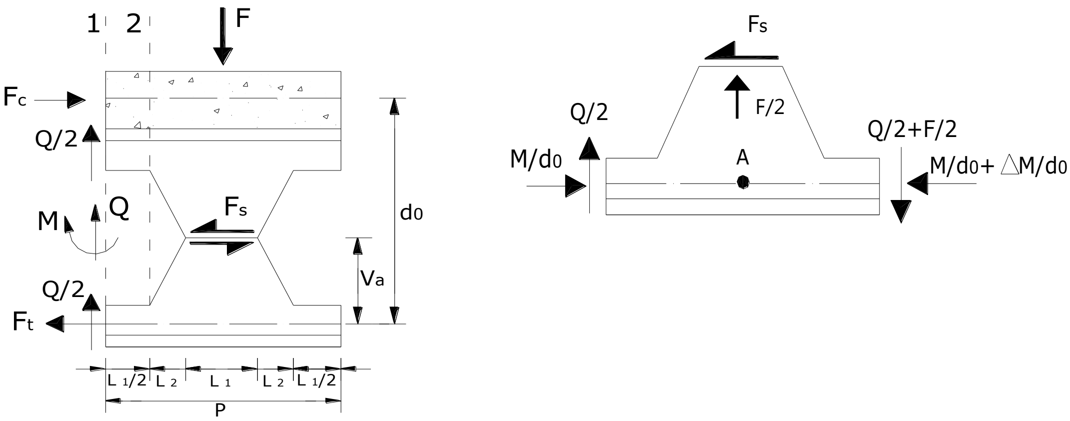

a) Forces acting in a beam section b) Equilibrium of the section

Figure 10: Forces distribution applied in the Model-02.

4 RESULTS AND DISCUTION

The ANSYS FE results presented in this paper are plotted together with the results from the analytical models proposed by Model-01 and Model-02 formulations as explained in the last section. It is noticed that the ANSYS stress are intermittent at the voids generated by the hexagonal openings in along the web span of the beam. The loading in the ANSYS program are increased load step by load step until the beam is unable to resist. Therefore, the stresses plotted corresponds to the onset of the collapse of the beam. In the plots, the equivalent stress from ANSYS runs are the von Mises (τ_{vM}) stress. The solid lines representing Model-01 and 02 are colored, respectively, in blue and red. This von Mises equivalent stress (Saeed (1995), Hearn (1977)) at the weld region takes into account the normal (σ) and shearing (τ) stress at the weld string and can be expressed by the following equation.

$$\sigma_{vM} = \sqrt{\sigma^2 + 3.\tau^2} \tag{9}$$

The results presented here shows the effect of the NA position on the weld stress. For all the analyses an original IB rolled steel beam W200x15 is used to produce the HoIB section used in the composite concrete-steel beam. The CS assumed in the analyses has thickness tc =10 cm and is made of concrete with f_{cck} = 25 MPa. The holes are manufactured as explained in section 1.1 to reach the maximum depth - see Equations (1) and (2) (which means n=0,5 and h_f = 26,667 cm).

4.1 The effect of the NA change on the weld stress

The effect of the NA position is studied considering three different beam spans and one size of the hexagonal hole (L_1 = 2.L_2, h_f = h_{p1}/2 (n=0,5) - see Figure-2). The beam span (L) is chosen following the recommendations presented by Veríssimo (1998) where L/h_{p1} varies in the range 10 to 30. In this paper, the L/hp1 is such that the number of hexagonal holes along the span is even. In this case, the weld string at the web and at the middle of the HoIB span will be under the maximum bending moment. The maximum shearing stress will be at the ends of the beams. In all cases, the distance between the first and the last holes to the beam ends is constant.

Span Variation (9-analysis)		
L_1 = 2.L_2,= h_f/2 ; n = 0,5		
NA =2 cm	NA = 6 cm	NA =10 cm
L/ h_{p1} = 10; L/ h_{p1} = 19; L/ h_{p1} = 29,5		

Table 3: Analyses applied in the study of weld stress.

4.1.1 Results for NA located at ≈2 cm from the top

The characterization of the beam is this case is presented in Table-4. Considering the plots of the stress in Figure 11 and Figure 12, it is clear that the stresses at the weld string diminish towards the center of the beams. The high stress value in the weld is next to the support region – area under great influence of the shearing stress. Model-01 shows good result for the first analysis (L/h_{p1}=10), while Model-02 is not so good for L/h_{p1}=10, but reasonable for the other L/hp1 values. Also observe that Model-02 is always right above the FEM results.

L/h_{p1}	10	19	29,5
b_e (cm)	66,13	82,67	82,67
Dist. "d_o" (cm)	22,08	22,33	22,33
Load (kN/cm)	1,2166	0,2928	0,1341
Force (F- kN)	24,33	5,86	2,68

Table 4: Structure values applied when NA = 2 cm.

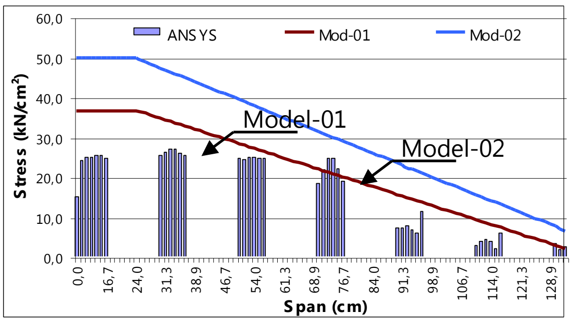

a) Analysis- 01 – L/ h_{p1} = 10

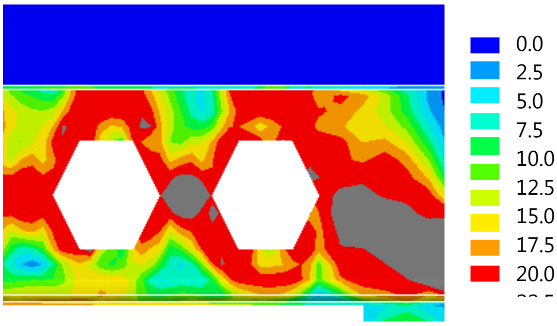

a.1) Stress state (kN/cm^2)

Figure 11: Stress in the composite beam for NA = 2 cm (L/ h_{p1} = 10)

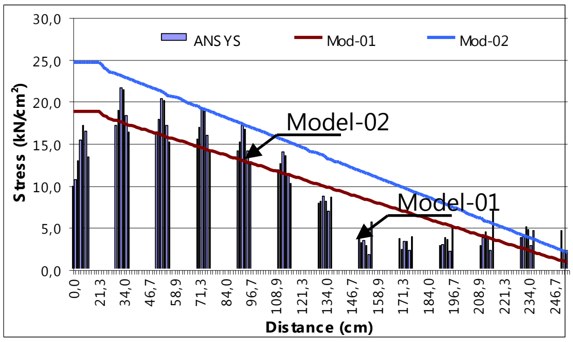

b) Analysis- 02 – L/ h_{p1} = 19

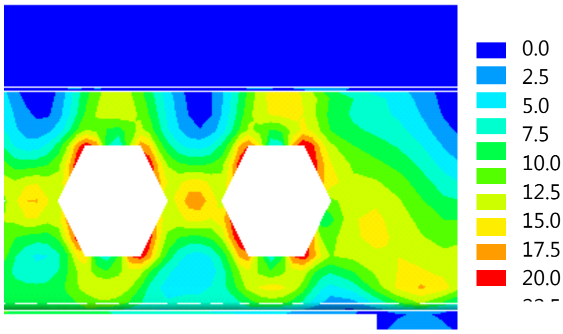

b.1) Stress state (kN/cm^2)

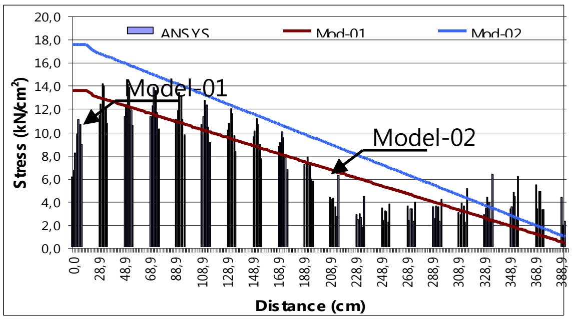

c) Analysis- 03 – L/ h_{p1} = 29.5

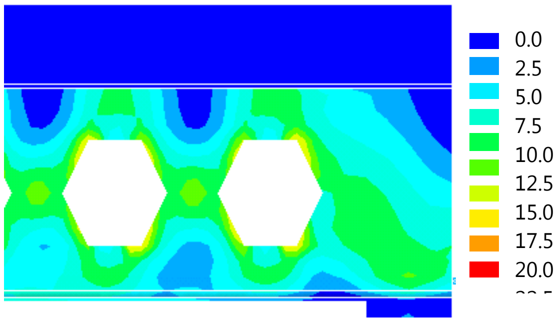

c.1) Stress state (kN/cm^2)

Figure 12: Stress in the composite beam for NA = 2 cm

4.1.2 Results for NA located at ≈6 cm from the top

In this case, the characterization of the beam is presented in Table-5. Examining the plots in Figure 13, it is noticed that the stresses behave as in the case before (4.1.1).

L/h_{p1}	10	19	29,5
b_e (cm)	27,55	27,56	27,56
Dist. "d_o" (cm)	20,33	20,33	20,33
Load (kN/cm)	1,0645	0,2799	0,1138
Force (F- kN)	21,29	5,60	2,28

Table 5: Structure values applied when NA = 6 cm.

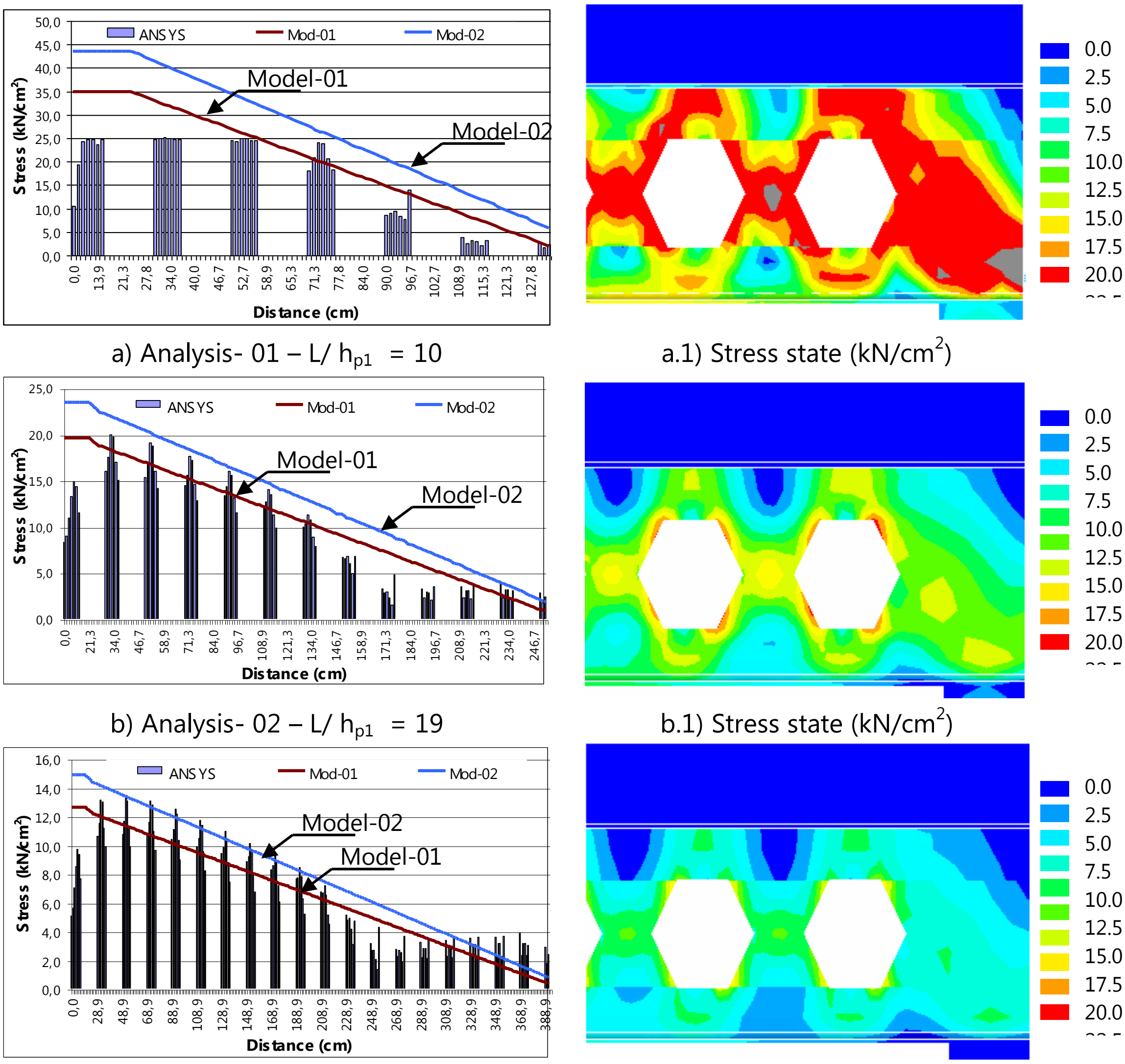

a) Analysis- 01 – L/ h_{p1} = 10 a.1) Stress state (kN/cm^2)

b) Analysis- 02 – L/ h_{p1} = 19 b.1) Stress state (kN/cm^2)

c) Analysis- 03 – L/ h_{p1} = 29.5 c.1) Stress state (kN/cm^2)

Figure 13: Stress in the composite beam for NA = 6 cm

4.1.3 Results for NA located at ≈10 cm from top and at the interface CS/HoIB

The beam is characterized in Table 6. The plots in Figure 14 compared to the plots in Figures 11 to 13 show the same behavior as in the cases analyzed before. However, comparing FE results and analytical formulations, for this position of NA and L/hp1 = 29,5, Model-02 underestimates the weld stress. Examining Figures 11, 12, and 13, note that weld stresses go under a reduction as the position of the NA moves towards the upper flange of the HoIB.

L/h_{p1}	10	19	29,5
b_e (cm)	16,53	16,53	16,53
Dist. "d_o" (cm)	18,33	18,33	18,33
Load (kN/cm)	0,9709	0,2520	0,1023
Force (F- kN)	19,42	5,04	2,05

Table 6: Structure values applied when NA = 10 cm

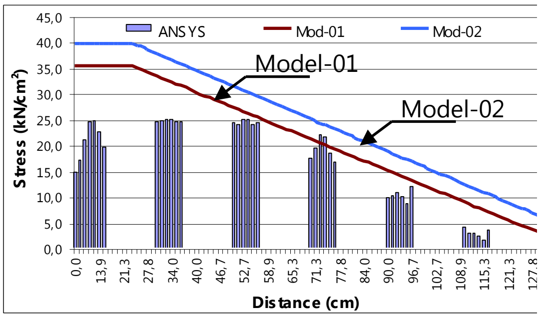

a) Analysis- 01 – L/ hp1 = 10

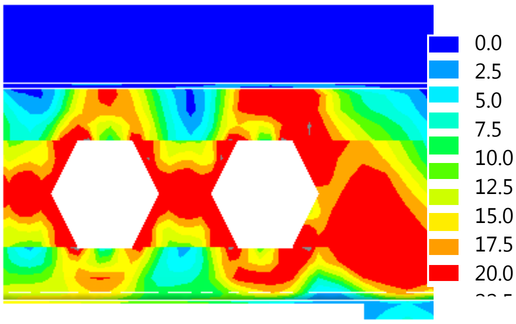

a.1) Stress state (kN/cm2)

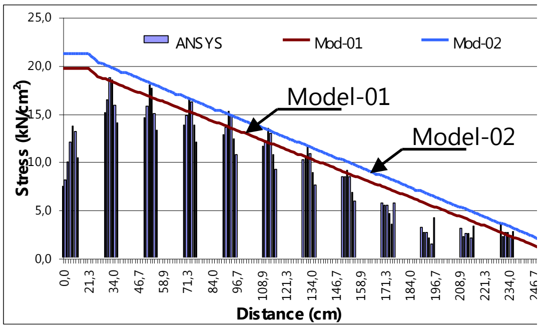

b) Analysis- 02 – L/ hp1 = 19

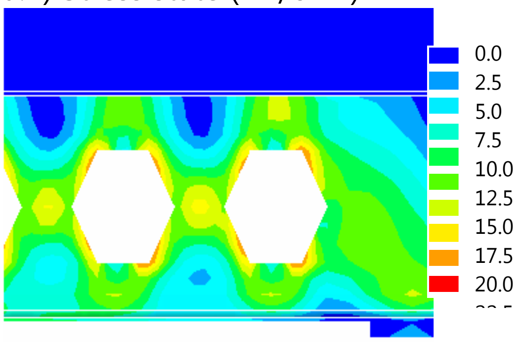

b.1) Stress state (kN/cm2)

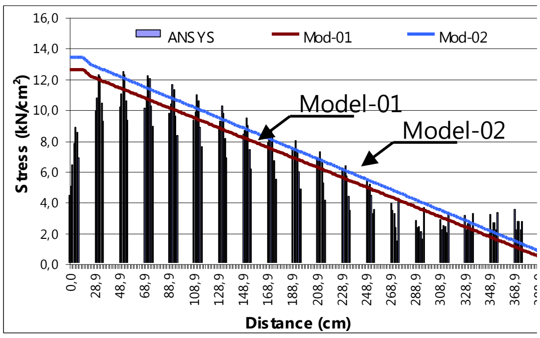

c) Analysis- 03 – L/ hp1 = 29,5

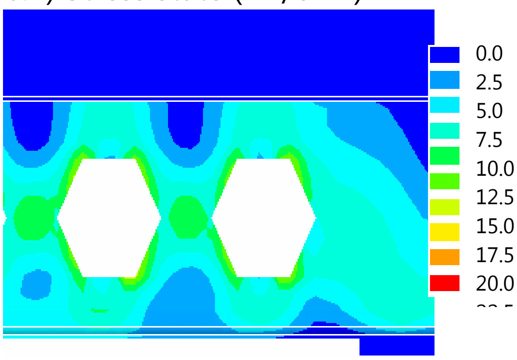

c.1) Stress state (kN/cm2)

Figure 14: Stress in the composite beam for NA = 10 cm

5 CONCLUSION

This article studies the stresses acting in the weld string at the web of composite concrete-steel beams with hexagonal holes on the webs. The beams considered in this work are simple supported at the ends and under uniform loading. Stress analysis from FE results and analytical formulations proposed in this article are presented along the paper. The stress results demonstrate that the weld string under higher stress is always near the ends of the beam next to the supports, where the shear stress is at maximum and bending moment is at minimum. The values of the weld stresses decrease in the direction of the middle of the beam span, where the bending moment is at maximum and the shear stress is at minimum. It is observed that the weld stresses decrease as the NA position in the concrete slab goes towards the HoIB upper flange. This fact also produces a reduction in the bending moment strength causing also a decline in the values of the weld stress. Moreover, for short spans, high shearing stress takes place at the support region causing stress increments at the weld string. This is explained because for constant bending moment value (M) at the middle of the beams ($M=ql^2/8$), the beam with shorter span ($l_1<l_2$) is under higher uniform loading ($q_1>q_2$). For this reason, higher shearing stress at the support regions are observed. With respect to the proposed analytical models, and according to the range of beam spans analyzed here, Model-01 presents good results for short beam spans, L/h_{p1} =10, while Model-02 is good for other spans in the range $10 < L/h_{p1} < 29{,}5$.

References

Cimadevila, J.C., Gutiérrez, E.M., Rodríguez, J.A.V., *Vigas Alveoladas*, Bellisco Ediciones Tecnicas y Científicas, Espain, 2000.

N.B.R-8800, *Projeto e Execução de Estrutura de Aço e de Estruturas Mistas Aço-Concreto de Edifícios*, Brasil, 2003

MacGregor, J.G., *Reinforced Concrete Mechanics & Design*, Prentice Hall, United States of America, 1992.

Galambos, T.V., Lin, F.J., Johnston, B.G., *Basic Steel Design with LRFD*, Prentice Hall, United States of America, 1996.

"ANSYS user manual (Revision 5.2, reference manual", United States of America, 1995.

Saeed, M., *Finite Element Analysis*", Prentice Hall, United States of America, 1995.

Hearn, E.J., *Mechanics of Materials*", Pergamon Press, United States of America, 1977.

Veríssimo, G.S., Fakury, R.H., Design of Steel and Composite Beams with Web Openings, *Journal of Constructional Steel Research*, 46:1-3, Paper No. 108, 1998.